Uniwersytet Wrocławski

Numerical study of fabrication tolerances for dielectric laser acceleration (DLA) structures

Andrzej Szczepkowicz

Institute of Experimental Physics
University of Wroclaw

EAAC 2019, Elba
Working group 3

Uniwersytet Wrocławski

Presentation outline

1. Literature on tolerances in DLA

2. Simple numerical models:
– double column setup
– Bragg mirror

3. Adjusting of a fabricated structure?
– electro-mechanical: piezoelectric effect
– electro-optical: Pockels effect

4. Conclusions

Woodpile accelerating structure, fabrication tolerance

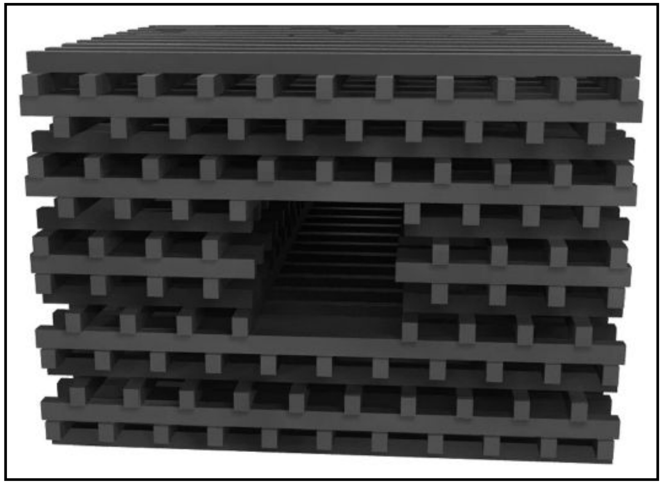

J. England *et al.*, Rev. Mod. Phys. 86, 1337 (2014);
B. Cowan *et al*., IPAC2010 proceedings;

"Fabrication of 17-layer woodpile accelerator structures was successfully achieved using the layer-by-layer approach [...]. Fabrication tolerances were <u>within 5–8% of the layer thickness</u>, rod width, layer-to-layer alignment, and taper angle. Final alignment of the two half structures reveals a <u>one-third period offset</u>. Improved accuracy and automation in the alignment system is important for future fabrication runs."

Dual grating structure sensitivity analysis, F. Mayet et al. 2018

F. Mayet *et al.*, *First order sensitivity analysis in dual grating type dielectric laser acceleration structures*, Proceedings of IPAC2018

- Influence of laser beam parameters and input electron beam parameters on output beam parameters

partial variances is used. This method is based on a large number of Monte Carlo runs of a given model. This way also numerical models can be used. The resulting sensitivity measure is refered to as the *first order sensitivity index* of a given input parameter to the system. It is given by

$$S_i = \frac{\mathrm{V}_{a_i}(\mathrm{E}_{\sim a_i}(f(\mathbf{a})|a_i))}{\mathrm{V}(f(\mathbf{a}))} \in [0,1], \qquad (4)$$

where – sticking to the literature – V is the variance, E the expectation value and $\sim a_i$ means "all but a_i" (cf. [3]). The numerator can be read as "the variance of the expectation value of $f(\mathbf{a})$ for fixed (known) a_i". One additional advantage of this measure is the fact that the whole configuration space is explored instead of focusing on one fixed a_i. In

[A. Saltelli, *Global Sensitivity Analysis: The Primer*, Wiley, Chichester, (2008).]

"Finally it has to be noted that this kind of analysis does not have to be based on simulations. It can also be performed on experimental data. If the data aquisition of all relevant machine parameters is time synchronized, recorded data then corresponds to the Monte Carlo runs of a given model."

Uniwersytet Wrocławski

Photonic bandgap fiber accelerators, tolerance studies, L. Genovese et al. (2019)

Abstract

Laser-driven hollow core photonic bandgap (PBG) fibers were proposed by Lin in 2001 as high-gradient accelerators. The central defect in the transversely periodic lattice supports an accelerating mode for synchronous acceleration in the ultra-relativistic regime. The optical frequencies in such dielectric laser accelerators motivate a sensitivity and tolerance study to overcome manufacturing imperfections. Finally we discuss the propagation characteristics of Lin-fibers and find that small-bandwidth (~ns) pulses would be needed for efficient acceleration over longer distances.

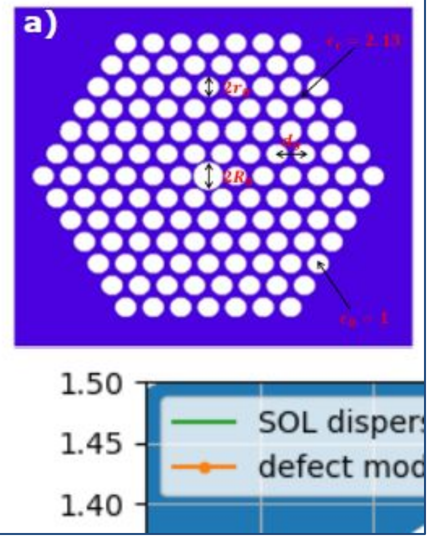

In this paper we have presented a tolerance study assuming realistic manufacturing imperfections and showing that the geometrical PBG fiber properties play a crucial role for getting and confining the optimal accelerating mode into the defect. Moreover, we find a tolerance range of 10% in which the mode properties in the fiber can be recovered by tuning the laser wavelength. Finally, we have pointed out that a

Uniwersytet Wrocławski

Dual pillar grating with a Bragg mirror, P. Yousefi *et al.* 2019

P. Yousefi *et al*, EAAC2017 proceedings,

P. Yousefi *et al*, Opt. Lett. 44, 1520 (2019).

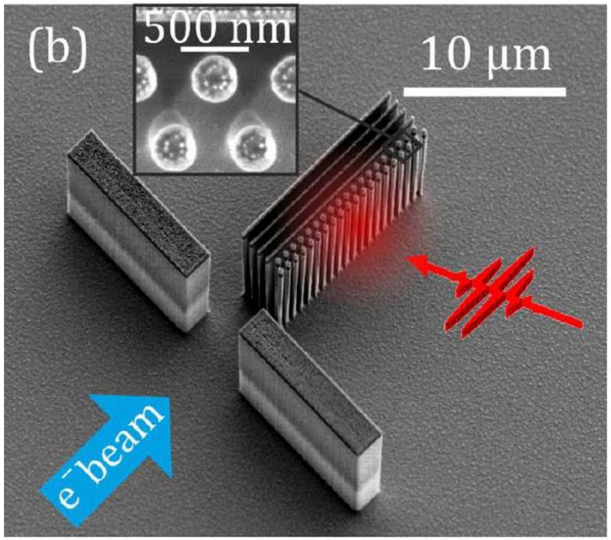

"Our final structures have a standard deviation of 10 nm from the designed geometry" [~0.5% of the laser wavelength] [local defects?]

"We fabricated two sets of structures [...]. The relative difference between geometrical dimensions of the fabricated structures is 0.8%."

A numerical model: double column DLA segment

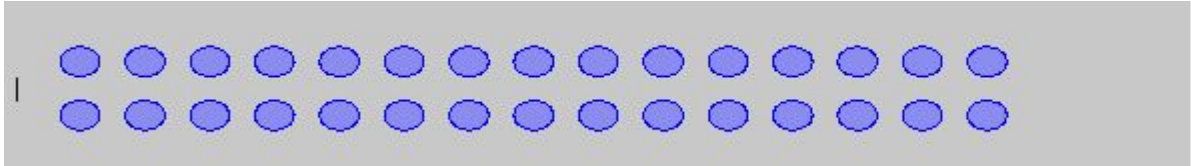

- Geometry and laser parameters from D. Black *et al.*, *Laser-driven electron lensing in silicon microstructures*, PRL 122, 104801 (2019)

  15 pairs of Si columns

  electron velocity beta = 0.525
  laser wavelength = 1.95 um, vacuum gap = 0.375 um
  laser field from two sides, amplitude E0 = 300 MV/m

- focal length = 18.4 um

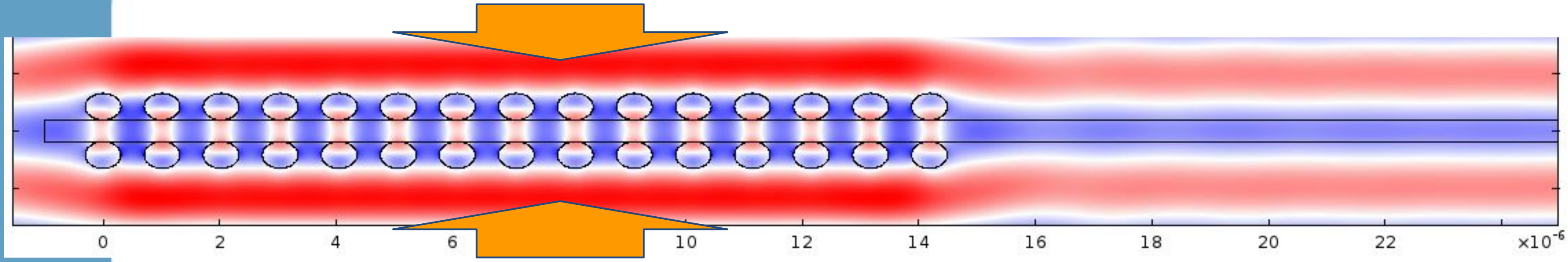

Numerical particle tracking approaches

- Full PIC code
- Often used alternative: a code to calculate field, another code to track particles
- This work: all in Comsol (RF Module + Particle Tracing Module)
- Particle tracking approaches based on the transfer properties of a DLA unit cell, utilizing quasi-periodicity of DLA structures.
  - U. Niedermayer et al., IPAC2017 Proceedings;
    U. Niedermayer et al., PRAB 20, 111302 (2017).
  - W. Kuropka, et al, IPAC2017 Proceedings;
    F. Mayet et al, IPAC2017 Proceedings
  - A. Szczepkowicz, PRAB 20, 081302 (2017);
    A. Szczepkowicz, EAAC2017 Proceedings
  - Beware of boundary effects

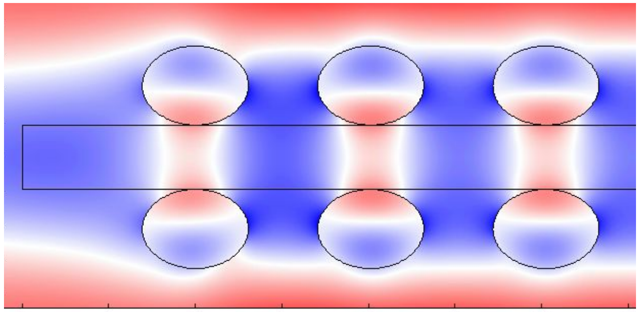

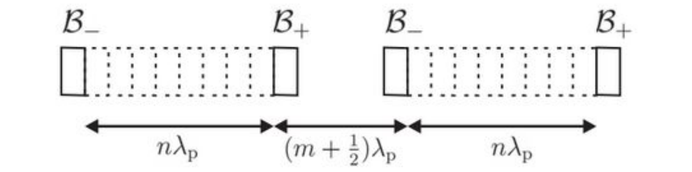

FIG. 8. Boundary field effects can be handled using boundary cells with corresponding $\mathcal{B}_\pm$ transfer functions.

A. Szczepkowicz, PRAB 20, 081302 (2017)

A numerical model: double column DLA segment
1. Sensitivity to column cross-section size

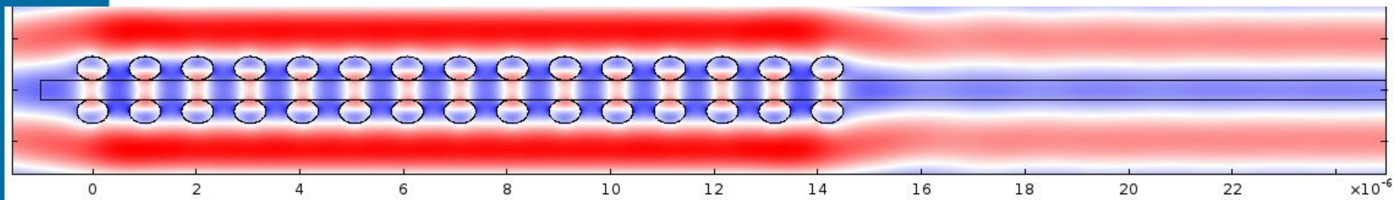

Trace space plots

Design geometry

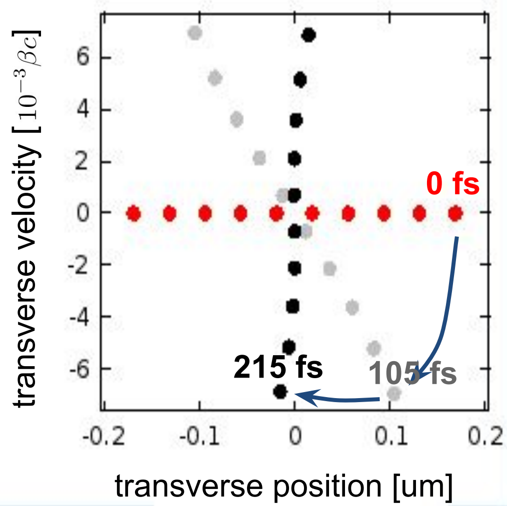

focal length = 18.0 um

Modified geometry thinner columns (−10%)

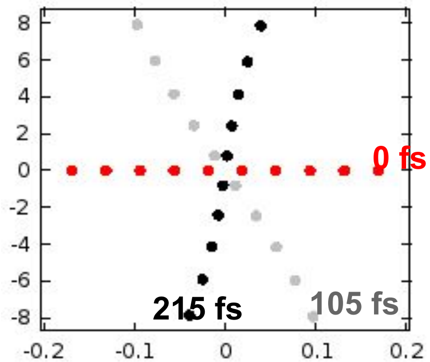

focal length = 14.8 um

Modified geometry thicker columns (+10%)

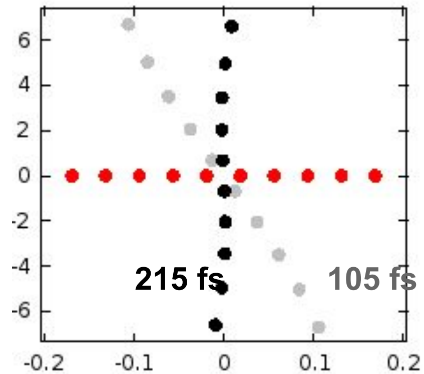

focal length = 18.8 um

2. Sensitivity to vacuum channel width
3. Sensitivity to laser phase mismatch

Design geometry,
f=18.0 um

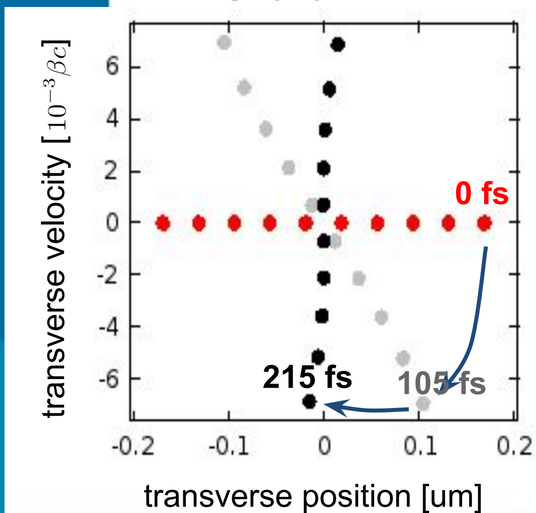

Narrower vacuum channel (−10%)
⇒ f = 16.5 um

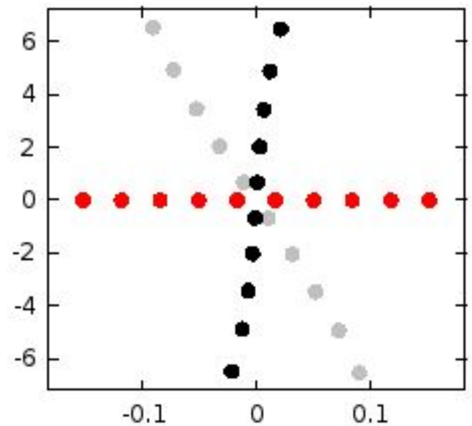

Wider vacuum channel (+10%)
⇒ f = 19.7 um

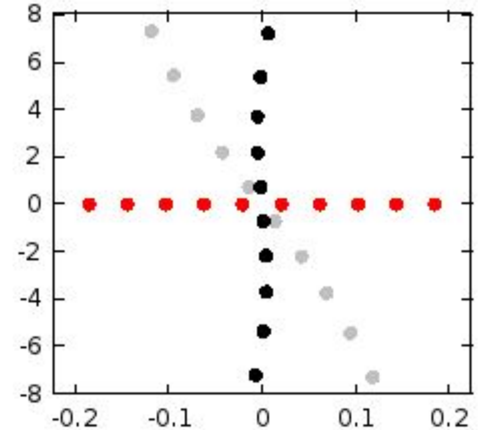

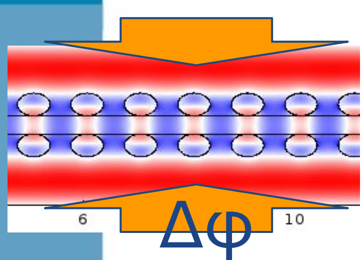

…

Laser#1 phase change (−30°)
⇒ f = 22.2 um and
focus transverse shift −26 nm

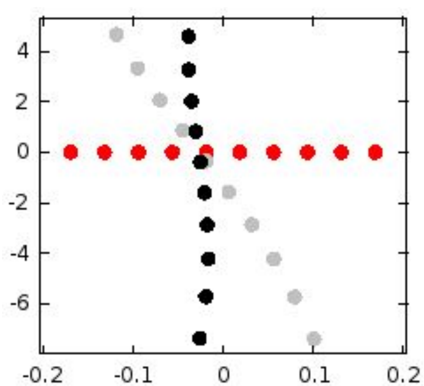

Laser#1 phase change (+30°)
⇒ f = 19.6 um and
focus transverse shift −8 nm

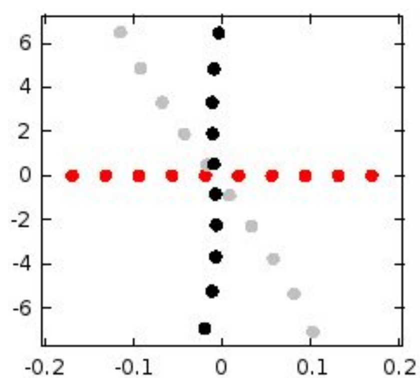

A numerical model: Bragg mirror
Vacuum/Si interface shifts

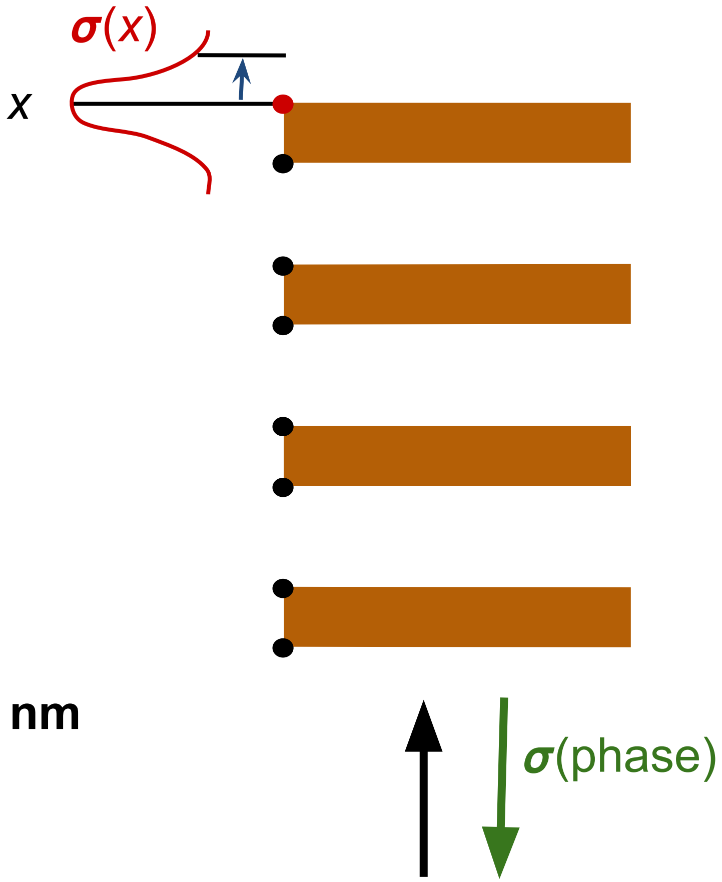

λ = 2 um
λ / 4 = 500 nm

Bragg mirror
Systematic vs. random interface shifts

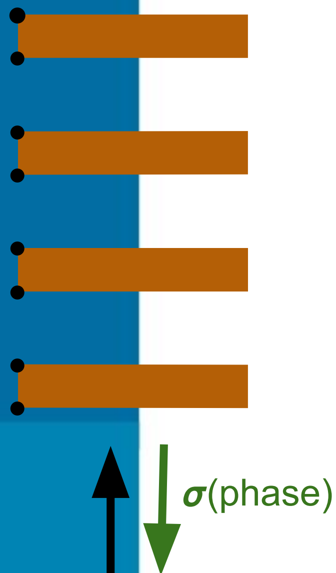

λ = 2 um
λ / 4 = 500 nm

First step – equal interface shifts

$$(\Delta x_1, \Delta x_2, \ldots \ \Delta x_8) = (\Delta x, \Delta x, \ldots, \ \Delta x)$$

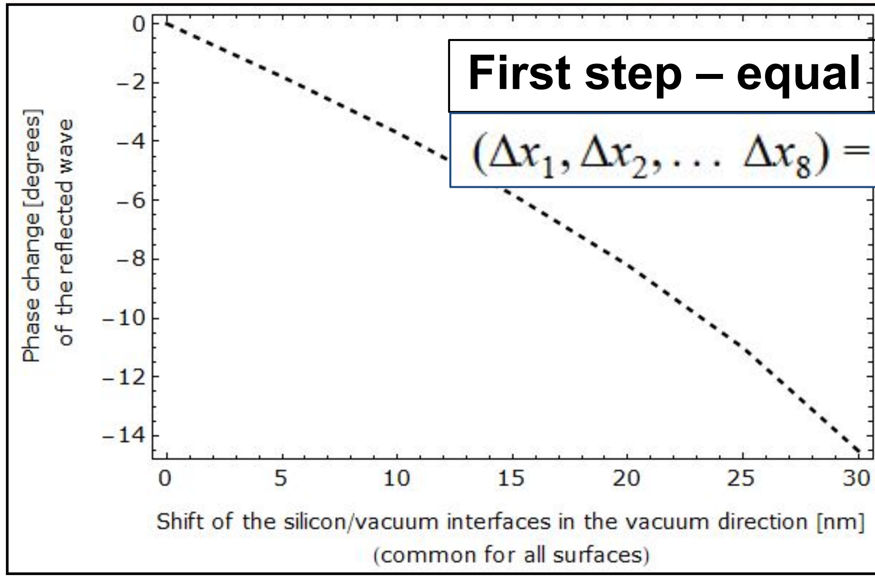

Random, independent interface shifts, 30 samples

$(\Delta x_1, \Delta x_2, \ldots \ \Delta x_8)$ = random set

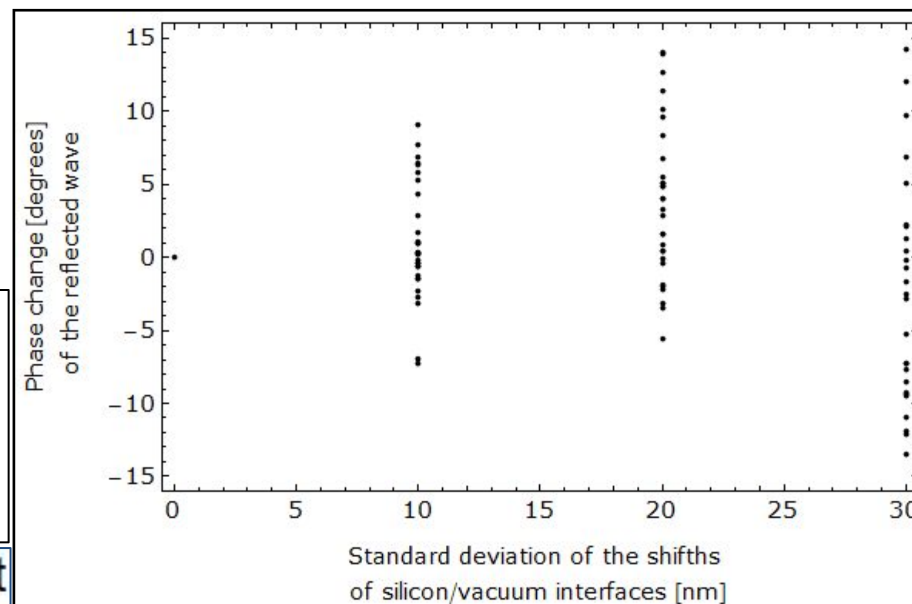

Bragg mirror
Shifting only one interface

i8	i7	i6	i5	i4	i3	i2	i1	R (1)	arg(e...	abs(e...
0	0	0	0	0	0	0	30	0.99978	-0.35824	0.99989
0	0	0	0	0	0	30	0	0.99978	-10.15...	0.99989
0	0	0	0	0	30	0	0	0.99978	-0.02929	0.99989
0	0	0	0	30	0	0	0	0.99978	-0.8596	0.99989
0	0	0	30	0	0	0	0	0.99978	-0.00145	0.99989
0	0	30	0	0	0	0	0	0.99978	-0.07166	0.99989
0	30	0	0	0	0	0	0	0.99978	0.00142	0.99989
30	0	0	0	0	0	0	0	0.99978	-0.00505	0.99989

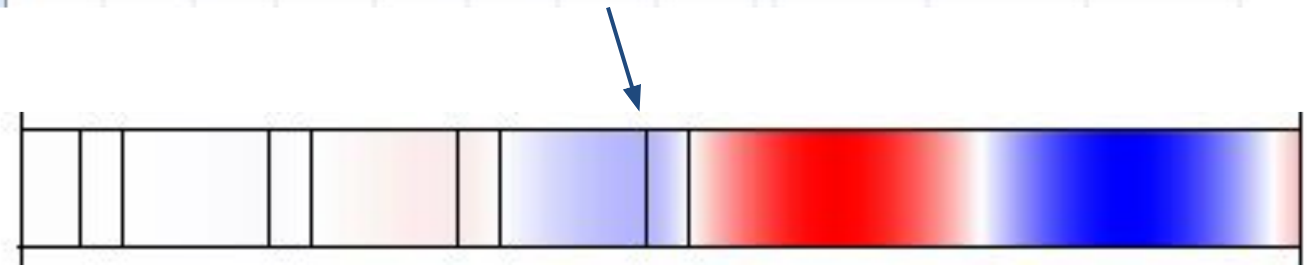

For the phase of the reflected wave, the position of the second interface is crucial ("back of the first layer").

Optical anisotropy of crystalline silicon? Tolerance to uncertainty of *n*?

[Yousefi *et al*. 2019] use “phosphorus-doped Si<100>” ⇒ crystalline Si

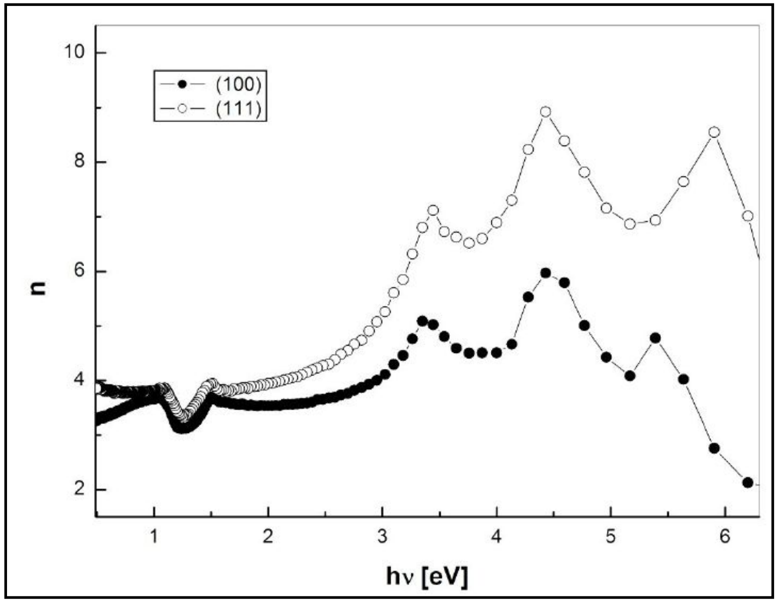

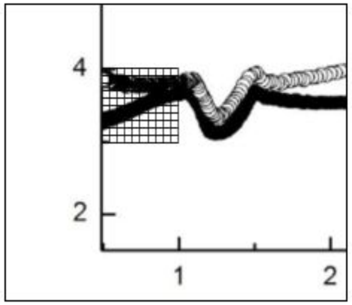

⇒ **n= 3.35, 3.80**

M. El-Nahass and H. Ali, *Estimation of optical parameters of silicon single crystals with different orientations*, Materials Science-Poland, 37, 65 (2019)

⇒ *n* = 3.35, 3.80, 13% difference at 2 um (hν = 0.62 eV)

Amorphous silicon at 2 um: *n* = 3.45 (3.51 @ 600 K)
https://refractiveindex.info/?shelf=main&book=Si&page=Li-293K

Post fabrication, in-situ tuning of DLA structures? Piezoelectric crystals? Piezoaligment?

shear piezos

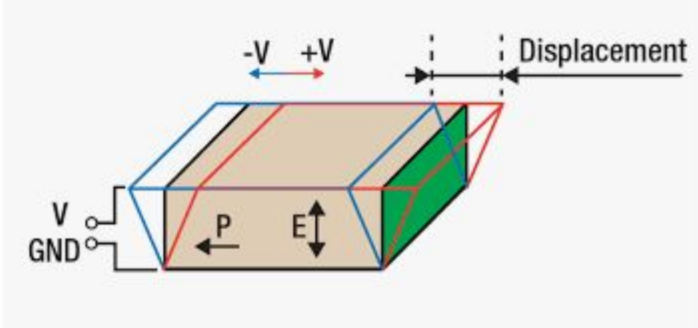

Low-Voltage Shear Piezoelectric Chips and Stacks
thorlabs.com

DLA section 1

DLA section 1

How to align DLA segments?

2018 Kozak *et al*, *Ponderomotive*... - Supplemental Material
“One translation stage in the ω1 interferometer is equipped with a piezo-crystal allowing to change its position with a precision of 10 nm.”

2018 Leedle *et al.* “The relative phase of the two lasers is controlled via a piezo-driven delay stage.”

Uniwersytet Wrocławski

A book on Scanning Tunelling Microscope
Tube scanners – "piezo tubes"

3 Technical Aspects of Scanning Probe Techniques

Bert Voigtländer

1.2 Tube Scanner

One central task in scanning probe microscopy is to position the scanning probe with an accuracy of less than one tenth of an Angstrom in all three dimensions. The tube scanner is the most widely used actuator element to move the probe tip or the sample in order to scan a surface (fine motion). This is due to its simple design, its high piezo constants and high resonance frequencies. It consists of a tube, made out of piezoceramics, which is covered inside and outside with metal, which acts as electrodes. The outer electrode is sectioned into four quadrants. The tube is poled in radial direction. One of the great advantages of the tube scanner is that motions in all three dimensions can be controlled by one very simple actuator element. A motion in z-

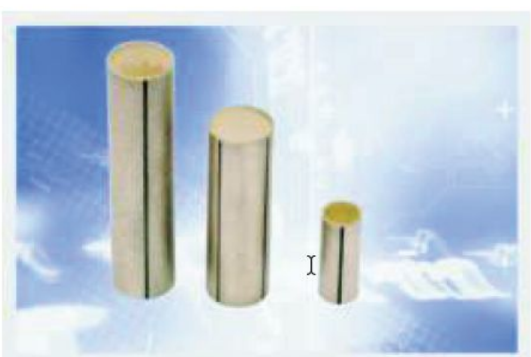

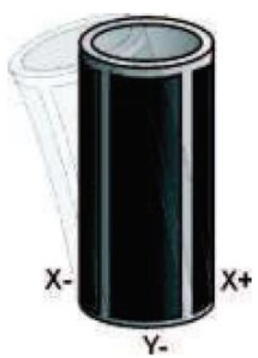

Electrooptical effect: Pockels effect in BTO/Si
Voltage-induced change of the refractive index

$BaTiO_3$ (Barium titanate, BTO)

nature materials

ARTICLES

https://doi.org/10.1038/s41563-018-0208-0

(2019)

Large Pockels effect in micro- and nanostructured barium titanate integrated on silicon

Stefan Abel[1,7]*, Felix Eltes[1,7], J. Elliott Ortmann[2], Andreas Messner[3], Pau Castera[4], Tino Wagner[5], Darius Urbonas[1], Alvaro Rosa[4], Ana M. Gutierrez[4], Domenico Tulli[6], Ping Ma[3]*, Benedikt Baeuerle[3], Arne Josten[3], Wolfgang Heni[3], Daniele Caimi[1], Lukas Czornomaz[1], Alexander A. Demkov[2], Juerg Leuthold[3], Pablo Sanchis[4]* and Jean Fompeyrine[1]

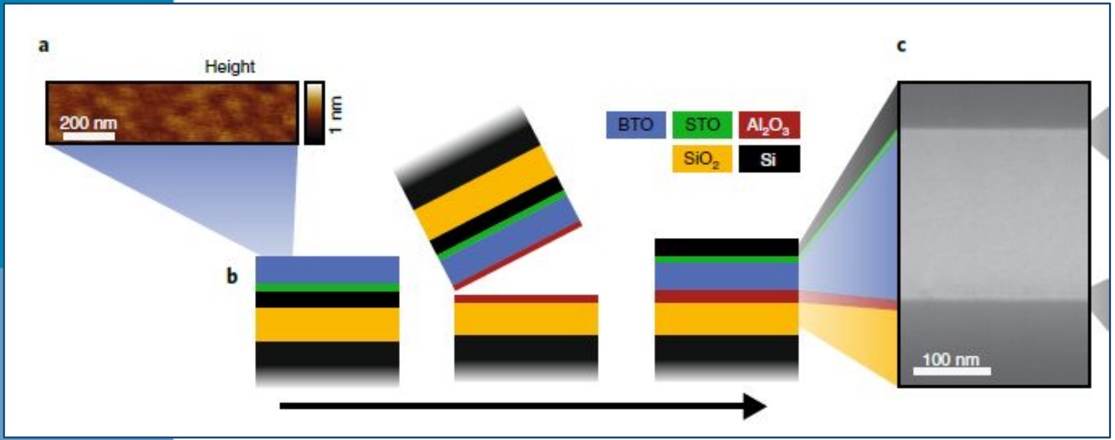

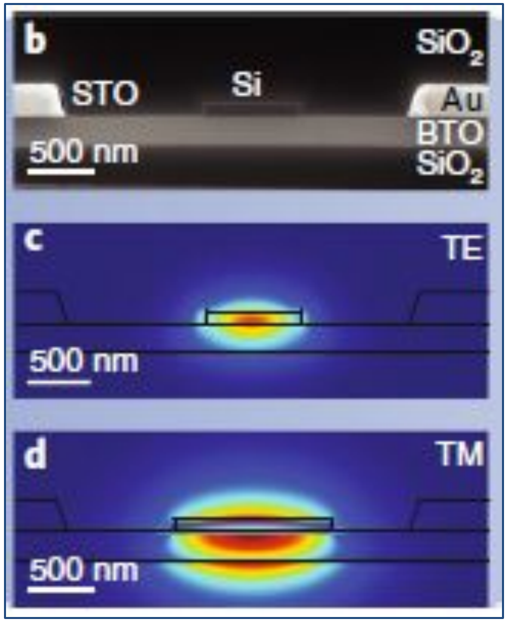

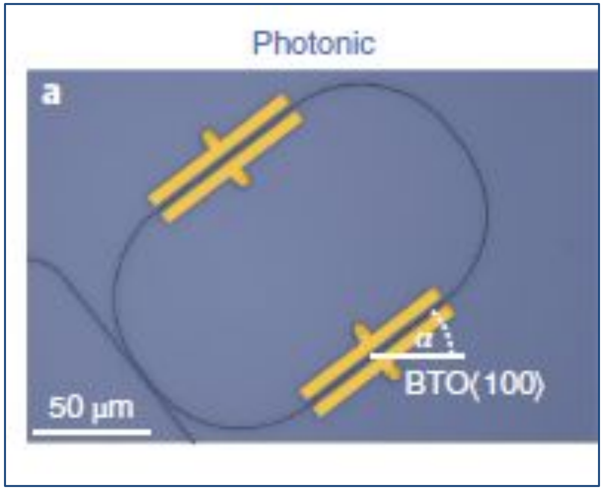

Electrooptical effect: Pockels effect in BTO/Si
Voltage-induced change of the refractive index

$BaTiO_3$ (Barium titanate, BTO)

refractive index ~2

largest coefficient of the Pockels tensor r_{42}~ 1 nm/V

Electric field-induced change of coefficients of the refractive index ellipsoid

$$\Delta\left(\frac{1}{n^2}\right)_i = \sum_{j=1}^{3} r_{ij} E_j, \quad i = 1\ldots6$$

$$\Delta n \sim \frac{n^3}{2}\Delta\left(\frac{1}{n^2}\right) \sim \frac{n^3}{2} r_{42} E_2$$

$$\text{e.g.} \quad \Delta n \sim \frac{2^3}{2} \cdot \frac{1\ \text{nm}}{\text{V}} \cdot \frac{10\ \text{V}}{200\ \text{nm}} = 0.2$$

[www.rp-photonics.com/pockels_effect.html]

Feedback beam tuning?

10. Transverse beam feedback

The beams in accelerators are inherently unstable. Many mechanisms are used in order to maintain the beam and its quality for many hours of circulation in the vacuum chamber. A crucial feedback system for the LHC is depicted in figure 26*a*. The transverse oscillations that appear at the onset of instability are measured in one location of the circumference by a suitable beam position monitor (BPM). This signal is processed electronically and a corrective 'kick' signal is generated, amplified and applied to the beam by a transverse electromagnetic field ('kicker'). Figure 26*b* shows the system as installed in the LHC tunnel.

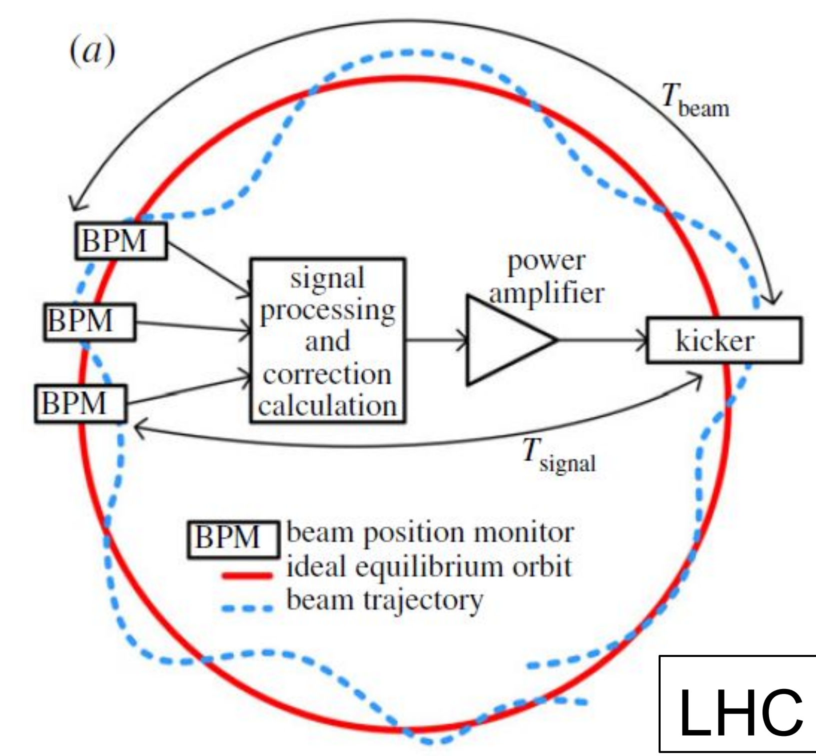

LHC

From: S. Myers, *The engineering needed for particle physics*, Phil. Trans. R. Soc. A370, 3887–3923 (2012)

On-Chip Laser Power Delivery System for Dielectric Laser Accelerators

Tyler W. Hughes,* Si Tan,† Zhexin Zhao, Neil V. Sapra, Kenneth J. Leedle, Huiyang Deng, Yu Miao, Dylan S. Black, Olav Solgaard, James S. Harris, Jelena Vuckovic, Robert L. Byer, and Shanhui Fan
Stanford University, Stanford, CA 94305

Yun Jo Lee and Minghao Qi
Purdue University, West Lafayette, IN 47907

(ACHIP Collaboration)

(Dated: September 14, 2017)

2017

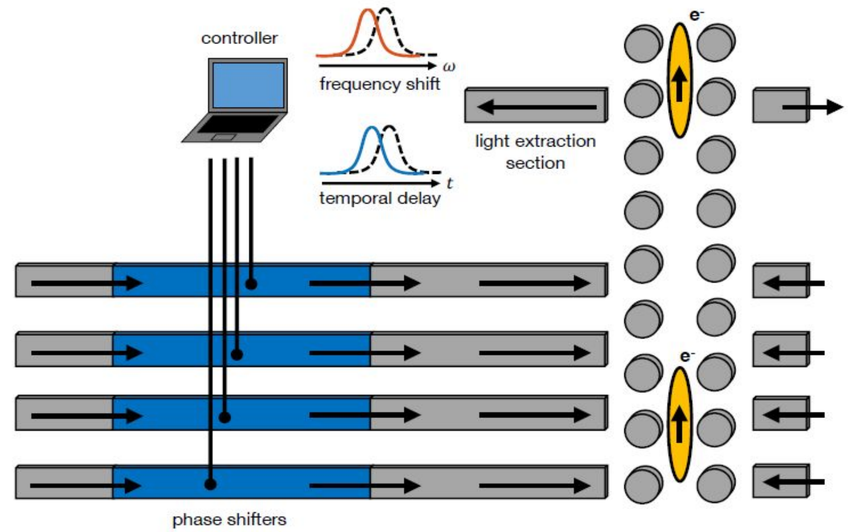

FIG. 7. Feedback system for automatic phase control. A dedicated light extraction section is added to the accelerator. Light is radiated from the electron beam transversing the DLA structures and the frequency content and/or timing of the light is sent to a controller. The phase shifts of each waveguide are optimized with respect to either the frequency or the delay of the signal. After several runs, the system should converge to stable operation.

Feedback structure tuning in DLA?

Structure tuning in DLA?

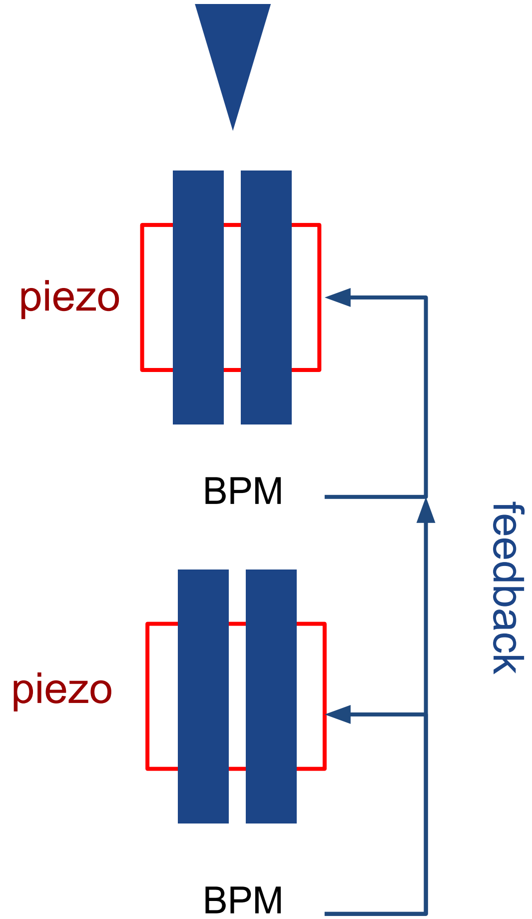

Uniwersytet Wrocławski

Tolerances in DLA: conclusions

1. Fabrication tolerances are not an issue for recent proof-of-concept DLA experiments utilizing short structures.

2. Fabrication constraints become tighter with increasing structure length, and post-fabrication adjustment of structures may become necessary:

– electromechanical: integrated shear piezo crystals? piezotubes?

– electrooptical: Pockels effect?

Acknowledgments

I am grateful to Joel England, Levi Schächter and Koby Scheuer for discussions on DLA,
to Oskar Warmusz for help with particle tracing in Comsol, to Marek Nowicki for his comments on piezo crystals, and to Janusz Przesławski for his comments on the electrooptical effects.

Today's DLA posters →

Uniwersytet Wrocławski

Today's poster session, 6 DLA posters

116. Frank Mayet, Status report on the dielectric laser acceleration experiments at the SINBAD/ARES linac

121. Thilo Egenolf, Transverse Beam Breakup Instability in Dielectric Laser Accelerators

159. Andrzej Szczepkowicz, Numerical calculation of the Purcell-Smith radiation from dielectric laser acceleration (DLA) structures

284. Stefanie Kraus, A compact UHV-compatible high-voltage supply for a small dielectric laser accelerator

318. Johannes Illmer, Alternating phase focusing in dielectric laser acceleration

331. Norbert Schönenberger, Generation and characterization of attosecond micro-bunched electron pulse trains via dielectric laser acceleration

Uniwersytet Wrocławski

…

…